Comparisons of six filters to remove high-frequency noises from interfered ECG

Jong Cook Park, Sang Hyun Park, Hye Jin Kim

Department of Anesthesia and Pain Medicine, Jeju National University School of Medicine, Jeju, Korea

Abstract

Background: An Electrocardiography obtained during operation is frequently contaminated with different types of noise. Noise sources such as an electrosurgical unit are obstacles that must be overcome by expert monitoring systems. We examined the six different low-pass filters (LPFs) designed to remove high frequency noises from an interfered ECG. Methods: ECG signals were collected using anesthesia monitors at a sampling rate of 300 Hz from 15 patients under general anesthesia. A high frequency sinusoidal noise signal of 38 Hz was added to the ECG signals to simulate - interfered ECG signals. Six LPFs (Window-sinc, 0% 6-pole , 0.6% 6-pole, 6% 6-pole, 16% 6-pole, and 26% 6-pole Chebyshev filter) were designed to remove the high frequency noise from the interfered ECG signal were constructed and their performance were tested. The one-way ANOVA was used to do statistical analysis on the differences between the LPFs. Results: In the correlation index and the reduction of magnitude of the high frequency noise, the Window-sinc filter was significantly better than the 6-pole Chebyshev groups (P < 0.01). In the 6-pole Chebyshev filters, rise in the ripple percentage increased noise reduction ratio but caused the distortion of QRS complex. Conclusions: We suggest the Window-sinc filter which performs better than 6-pole Chebyshev filters for removing noise from ECG signals. Further works are required to implement an optimized filter in real-time on an expert monitoring system. (J Med Life Sci 2010;7:37-43)

Key Words : Electrosurgery, Electrocardiography, Low frequency filter, Noise, Signal processing.

Introduction

Electrocardiogram (ECG) signals obtained during operation are critical for assessing patient status and conditions. Therefore, the measured signals must be accurate and free of contamination that may result from the presence of other signals within the surgical environment. These noises may be caused by respiratory activity, motion artifacts, or an electrical interference from medical instruments used for diagnosis and treatment[1-5]. Although abnormal noise signals are often removed using a band-pass filter (BPF) in the ECG monitoring system, the application of an electrosurgical unit (ESU) has often had influence on ECG signals[6]

A typical ESU involves an electrical circuit, which is composed of an electrosurgical generator, active electrode, patient, and patient return electrode[7]. The generator is able to produce a variety of electrical waveforms over a range of frequencies from 200,000 Hz to 3,300,000 Hz, resulting in desired effects such as cutting and coagulation[8-11] ECG

monitors contain a BPF, thus allowing the desired signal to be measured while removing the high-frequency noises. However, even if the primary ESU signal is removed by the BPF in the ECG monitor, lower frequency components may exist which can contaminate the ECG measurement. Therefore, if there are such low frequency noises which result from electromagnetic interference (EMI) and modulation, additional filtering is required to do accurate monitoring of ECG signals.

The purpose of this study is to test various filters and suggest a filter for removing noises from interfered ECG signals. Six different low-pass filters (LPFs) are constructed and tested, which include a Window-sinc LPF and five different 6-pole-type Chebyshev LPFs with a variety of ripple percentages, are then compared to evaluate and analyze their performance.

Materials and methods

This study was approved by the Ethics Committee at the institutional review board, and informed consent was obtained from every subject. 15 patients with American Society of Anesthesiologists physical status class I or II who were scheduled to undergo orthopedic operation or

Address for correspondence : Jong Cook Park
Department of Anesthesia and Pain Medicine, Jeju National University School of Medicine, 66 Jejudaehakno, 690-756, Jeju, Korea
E-mail : pjcook@jejunu.ac.kr

Table 1. Indications for Specific Diagnosis Test

| Age (yr)	49.0 ± 16.1
Sex (F/M)	12/3
ASA PS (I/II)	4/11
Body mass index (kg/m²)	24.0 ± 2.6
Operation site	
Knee	6
Pelvic cavity	4
Hip	3
Elbow	1
Shoulder	1

Gynecologic operation were used in this study (Table 1).

Monitoring parameters in the operating room included ECG (lead II), noninvasive systemic arterial pressure, pulse oximetry, end-tidal carbon dioxide and concentration of volatile anesthetic agents, ventilation pressure, and train-of-four ratio. All measurements were made with an anesthesia monitor (S/5 compact, Datex-Ohmeda Co., Helsinki,Finland).

General anesthesia was induced using fentanyl (1-1.5 μg /kg) and penthotal sodium (1.5-2.0 mg/kg). Tracheal intubation was facilitated by muscle paralysis with rocuronium (0.6-1.0 mg/kg). Anesthesia was maintained using a mixture of isoflurane (0.4-1.2%) and 50% N₂O/O₂. The rate of the respirator was set at 10 breaths/min, and tidal volume was initially set at 10 ml/kg and was then adjusted to maintain end-tidal CO₂ between 30-35 mmHg.

Disposable Ag-AgCl electrodes (Monitoring Electrode®, 3MKorea, Korea) were placed on the patient following proper skin preparation by cleaning with alcohol sponge. The ECG monitor was operated in monitoring mode, thus frequencies of 0.5-40 Hz were allowed. The ground plate for an ESU (ForceFX™-8C, Valleylab, USA: 390-494 kHz, 70-300 W/100-300 ohm) was placed on a site such as a buttock so that the current path from the surgical site to ground plate was far from chest. The computer with the data acquisition software, S/5 Collect (version 4.0, Datex-Ohmeda Co., Helsinki, Finland; 32-bit LabVIEW) was connected to the monitor through serial communication. ECG signals were collected and recorded from the anesthesia monitors using online S/5 Collect software at a sampling rate of 300 Hz.

After the operation was completed, the recorded ECG data were converted into ASCII code using S/5 Collect software in off-line mode. Since noise sources were present at various times during the procedures, only data in noise-free time sequences were kept for further analysis. Each ECG signal was saved in an ASCII code (true ECG) which contained 4,096 samples for approximately 14 sec (Figure 1A).
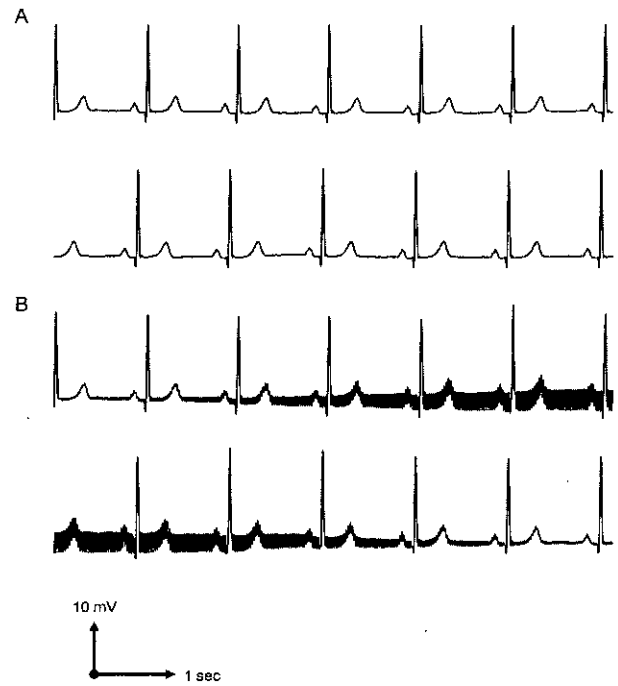
Figure 1. Typical ECG signals used in this work: (A) true ECG recorded at a rate of 300 samples per second; (B) simulated electrosurgical interference where 38 Hz frequency noise was added ECG signals.

To create an artificial noise, which, we assume, caused by ESU, we used a sinusoidal signal defined by

$$Noise[n] = A \cdot cos\left(2\pi f\frac{n}{f_s}\right) \times \left(0.54 - 0.46 \cdot cos\left(\frac{2\pi n}{N}\right)\right) \quad (1)$$

where, A is amplitude of 2, f is the frequency, f_s is the sampling frequency, n is 0, 1, 2, ⋯, 4,095, and N is 4,096. The high frequency sinusoid is multiplied by Hamming window[12], resulting in a noise signal with 4,096 data points where the samples near the ends are reduced in amplitude.

When the sampling frequency is 300 Hz, the frequency response of the 38 Hz sinusoidal noise signal is located at the same position where many sinusoids, including 262 Hz, 338 Hz, 562 Hz, ⋯, 390,038 Hz and so on, appear in the frequency response because of sampling theorem (Fig. 2B) [12]. The frequency of the noise signal was set to 390,038 Hz, and another frequency was calculated to result in the same frequency when spectral analysis was performed by using Discrete Fourier Transform (DFT)[13]. The artificial noise signal was added to the true ECG to create an interfered ECG (unprocessed ECG, Fig. 1B).

Spectral analysis was used with the following steps: a) a set of ECG data containing 4,096 samples was divided into
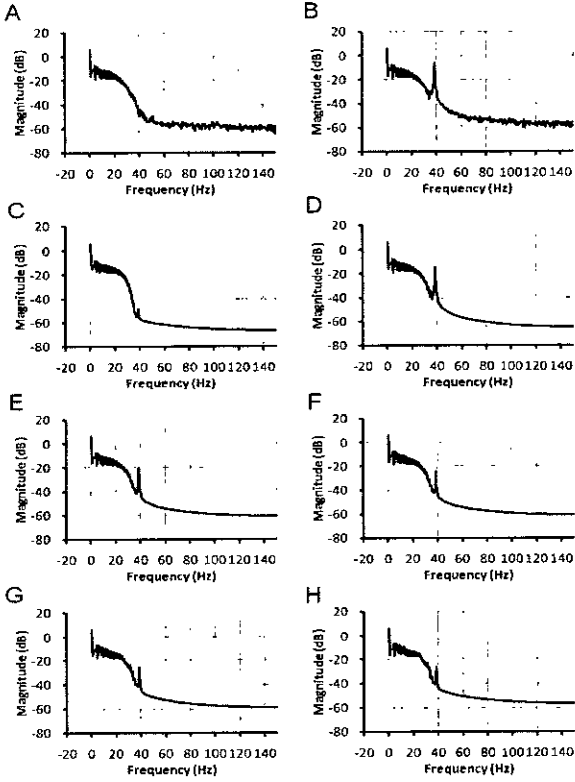
Figure 2. The frequency spectra of ECGs in the same patient are shown, The horizontal axis frequency in Hz and the vertical axis os magnitude in dB: (A) true ECG; (B) ECG to witch 38Hz noise was added; (C) ECG filtered by Window-sinc filter; (D) ECG filtered by 0% 6-pole Chebyshev filter; (E) ECG filtered by 0.6% 6-pole Chebyshev filter; (F) ECG filtered by 6% 6-pole Chebyshev filter; (G) ECG filtered by 16% 6-pole Chebyshev filter; (H) ECG filtered by 26% 6-pole Chebyshev filter.

8 segments consisting of 512 samples, b) each segment was analyzed using DFT and the magnitude of each segment was averaged in the frequency domain[12]. Results from spectral analysis of the true and unprocessed ECG are shown in Fig. 2.

In order to remove the interfered noise signal from the contaminated ECG, we considered the 2 types of LPFs: Window-sinc filter and 6-pole Chebyshev filters with varying ripple percentage. The filter design was carried out using using a spreadsheet program (Microsoft Excel, version 12).

The filter kernel of the Window-sinc filter was calculated by

$$h[i] = K \frac{sin\left(2\pi f_c\left(i - \frac{M}{2}\right)\right)}{i - \frac{M}{2}} \times \left(0.42 - 0.5\,cos\left(\frac{2\pi i}{M}\right) + 0.08\,cos\left(\frac{4\pi i}{M}\right)\right) \quad (2)$$

where the constant, K, is chosen to provide unity gain at zero frequency; the cutoff frequency, f_c , is expressed for

the sampling rate, a value between 0 and 0.5; the length of the filter kernel, M, is an even integer; and the sample number, i, is an integer that runs from 0 to M. Also, the sinc function was multiplied by Blackmann window to reduce the abruptness of the truncated ends of sinc function. The equation $h[i]=2\pi f c K$ is substituted when i is equal to $M/2$.

The cutoff frequency was set to 0.11 because the sinusoidal signal results in 0.127 in fraction of sampling rate when a sinusoidal signal has 38 Hz at the sampling frequency of 300 Hz, and filter length was set to 128 to have the bandwidth of 0.03125 according to the approximation:

$$M \approx \frac{4}{BW} \quad (3)$$

where BW is the width of the transition band.

The ripple for one of the 6-pole Chebyshev filters was set to 6% to provide the same roll-off as the Window-sinc filter. The ripples for the other filters were set to 0%, 0.6%, 16% and 26% to investigate the effect of ripple on filter performance. Recursion coefficients of the ripples for the 6-pole Chebyshev 6 filters are shown in Table 2.

The 6-pole Chebyshev filters with 0%, 0.6%, 6%, 16% and 26% ripple were multiplied by the delta function ($\delta[n]$) to obtain a filter kernel for each filter using the following recursive equation:

$$\begin{aligned} y[n] &= a_0x[n] + a_1x[n-1] + a_2x[n-2] + a_3x[n-3] + a_4x[n-4] \\ &+ a_5x[n-5] + a_6x[n-6] + b_1y[n-1] + b_2y[n-2] \\ &+ b_3y[n-3] + b_4y[n-4] + b_5y[n-5] + b_6y[n-6] \end{aligned} \quad (4)$$

where $x[]$ is the input signal or delta function ($\delta[n]$), $y[]$ is the output signal and the a's and b's are recursive coefficients of the 6-pole Chebyshev filter.

Convolution summations were[13] performed between the unprocessed ECG and each filter kernel to obtain a processed ECG:

$$y[n] = \sum_{k=0}^{K-1} h[n] \times x[n-k] \quad (5)$$

where $h[n]$ is the filter kernel, $x[n-k]$ is the input signal such as contaminated ECG, and K is the length of the $h[n]$ sequence.

Each of the ECGs filtered by LPF was called, according to the filter used, as Window-sinc group, 0% 6-pole Chebyshev group, 0.6% 6-pole Chebyshev group, 6% 6-pole Chebyshev group, 16% 6-pole Chebyshev group, and 26% 6-pole Chebyshev group (Fig. 3). The remaining noise at 38 Hz in the frequency domain was confirmed by using DFT [13].

Table 2. The 6-pole Chebyshev Filters with Five Ripple Percentages.

Recursive coefficient	0% 6-pole Chebyshev group	0.6% 6-pole Chebyshev group	6% 6-pole Chebyshev group	16% 6-pole Chebyshev group	26% 6-pole Chebyshev group
a_0	5.5324545×10^{-4}	1.4945702×10^{-4}	9.1409494×10^{-5}	7.3518580×10^{-5}	6.6966660×10^{-5}
a_1	3.3194727×10^{-3}	8.9674209×10^{-4}	5.4845696×10^{-4}	4.4111148×10^{-4}	4.0179996×10^{-4}
a_2	8.2986818×10^{-3}	2.2418552×10^{-3}	1.3711424×10^{-3}	1.1027787×10^{-3}	1.0044999×10^{-3}
a_3	1.1064909×10^{-2}	2.9891403×10^{-3}	1.8281899×10^{-3}	1.4703716×10^{-3}	1.3393332×10^{-3}
a_4	8.2986818×10^{-3}	2.2418552×10^{-3}	1.3711424×10^{-3}	1.1027787×10^{-3}	1.0044999×10^{-3}
a_5	3.3194727×10^{-3}	8.9674209×10^{-4}	5.4845696×10^{-4}	4.4111148×10^{-4}	4.0179996×10^{-4}
a_6	5.5324545×10^{-4}	1.4945702×10^{-4}	9.1409494×10^{-5}	7.3518580×10^{-5}	6.6966660×10^{-5}
b_1	3.3388196×10^{0}	4.3020448×10^{0}	4.6406487×10^{0}	4.8113111×10^{0}	4.9046397×10^{0}
b_2	-5.0131758×10^{0}	-8.2149627×10^{0}	-9.5242541×10^{0}	-1.0222216×10^{1}	-1.0615332×10^{1}
b_3	4.2144528×10^{0}	8.8129905×10^{0}	1.0978438×10^{1}	1.2196340×10^{1}	1.2902113×10^{1}
b_4	-2.0700157×10^{0}	-5.5703831×10^{0}	-7.4666516×10^{0}	-8.5920874×10^{0}	-9.2632639×10^{0}
b_5	5.5906004×10^{-1}	1.9602863×10^{0}	2.8357136×10^{0}	3.3850132×10^{0}	3.7225190×10^{0}
b_6	$-6.4548636 \times 10^{-2}$	$-2.9954092 \times 10^{-1}$	$-4.6974486 \times 10^{-1}$	$-5.8306597 \times 10^{-1}$	$-6.5496137 \times 10^{-1}$

To make quantitative evaluation on filtering, we used two measures: (1) the noise reduction ratio (NRR) at 38 Hz and (2) the correlation coefficient (CR) between the true and filtered ECGs.

The NRR is calculated by

$$NRR\ (dB) = 20\ log\left(\frac{M_a}{M_b}\right) \tag{6}$$

where Ma is the magnitude of the 38 Hz noise in contaminated ECG (before filtering) and Mb is that after.

The CR was calculated for the central portion of ECG signal (containing 400 samples) between the filtered and contaminated EGSs using equation (7).

$$r_{xy} = \frac{\sum_{n=1}^{N}(x[n] - \bar{x})(y[n] - \bar{y})}{\sqrt{\sum_{n=1}^{N}(x[n] - \bar{x})^2 \sum_{n=1}^{N}(y[n] - \bar{y})^2}} \tag{7}$$

where $x[n]$ and $y[n]$ are respectively the ECGs before and after filtering.

The performance of the 6 filters was tested in terms of the two parameters NRR and CR. Statistical analysis was carried out using the one-way ANOVA. When the P-value is less than 0.05, significant differences were determined by using Least Significant Difference test. Microsoft Excel was used to analyze the results.
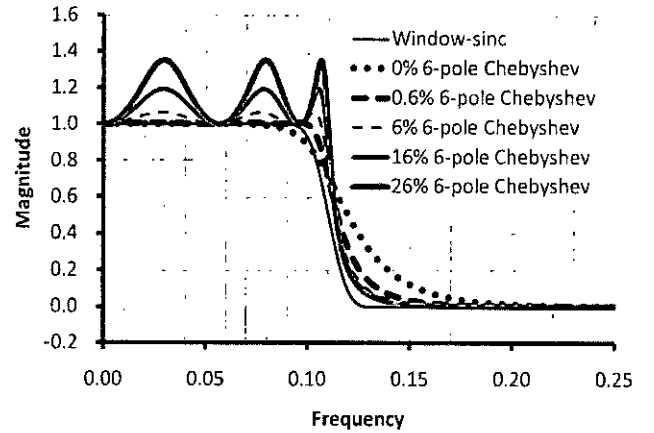
Figure 3. The frequency spectra of ECGs in the same patient are shown. The horizontal axis is frequency in Hz and the vertical axis is magnitude in dB; (A) true ECG; (B) unprocessed ECG; (C) processed ECG using Window-sinc filter; (D) processed ECG using 0% 6-pole Chebyshev filter; (E) processed ECG using 0.6% 6-pole Chebyshev filter; (F) processed ECG using 6% 6-pole Chebyshev filter; (G) processed ECG using 16% 6-pole Chebyshev filter; (H) processed ECG using 26% 6-pole Chebyshev filter.
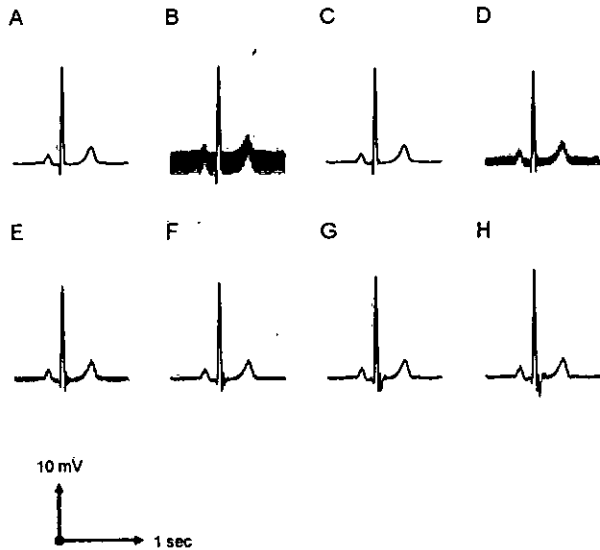
Figure 4. Comparison of the central portion of ECGs obtained under different conditions: (A) true ECG; (B) interfered ECG; (C) ECG filtered by Window-sinc filter; (D) ECG filtered by 0% 6-pole Chebyshev filter; (E) ECG filtered by 0.6% 6-pole Chebyshev filter; (F) ECG filtered by 6% 6-pole Chebyshev filter; (G) ECG filtered by 16% 6-pole Chebyshev filter; and (H) ECG filtered by 26% 6-pole Chebyshev filter.

Results

Fig. 4 shows the central portion of the true (A), contaminated (B) and filtered (C-H) ECG signals. The ECG signal filtered by Window-sinc in Fig. 2C does not show 38 Hz noise. As seen in Fig. 2D-H, in 6-pole Chebyshev filters, the noise level decreases with the extent of ripple, whereas the QRS complex is distorted more with the ripple percentage.

Table 3 displays the NRR and CR for each filter The Window-sinc group showed the noise reduction of 38.6 ± 3.0 dB, which was better than any of the other groups. For the 6-pole Chebyshev groups, the noise reduction increased from 8.7 ± 0.1 dB to 20.4 ± 0.3 dB as the ripple percentage rose from 0% to 26%.

The correlation coefficient is 0.998 ± 0.002 in the Window-sinc group which is significantly higher than the other groups. For the 6-pole Chebyshev filters, the correlation coefficient in 0% 6-pole Chebychev group is 0.964 ± 0.016 which is significantly lower than those in the 0.6% and 16% 6-pole Chebyshev groups. The correlation coefficient in 26% 6-pole Chebyshev group is 0.973 ± 0.008 which is significantly lower than that in the 0.6% 6-pole Chebyshev group (Table 3).

Table 3. Noise Reduction Ratio (dB) and Correlation Coefficient for Each Filter.

Group	Noise Reduction Ratio(dB)	Correlation Coefficient
Window-sinc	38.6 ± 3.0*	0.998 ± 0.002‖
0% 6-pole Chebyshev	8.7 ± 0.1†	0.964 ± 0.016‖
0.6% 6-pole Chebyshev	14.6 ± 0.2‡	0.983 ± 0.006**
6% 6-pole Chebyshev	18.0 ± 0.3§	0.982 ± 0.004
16% 6-pole Chebyshev	19.6 ± 0.3	0.981 ± 0.007
26% 6-pole Chebyshev	20.4 ± 0.3	0.973 ± 0.008

*: $P < 0.05$ vs. other groups. †: $P < 0.05$ vs. other groups. ‡: $P < 0.05$ vs. other groups. §: $P < 0.05$ vs. other groups. ‖: $P < 0.05$ vs. other groups. ¶: $P < 0.05$ vs. other groups. **: $P < 0.05$ vs. 26% 6-pole Chebyshev group.

Discussion

This study showed that the high frequency noise was successfully removed by the low pass filters tested, and it was observed that Window-sinc filter performed even better than the 6-pole Chebyshev filters. In the 6-pole Chebyshev filters, as the ripple was amplified, the noise was reduced but the QRS complex was distorted more.

When an ESU is used in cut mode, it is known that its waveform is almost a pure sinusoid[5]. Although most of the monitoring systems have anti-aliasing filters, ECG signal can be interfered by the noise from ESU because of EMI and modulation. We assumed that such a high frequency noise signal can be leaking during analog-to-digital converter (ADC).

When a continuous signal such as ECG is sampled using an ADC, frequencies above half the sampling frequency are reflected in the lower half of the spectrum. The frequency $f_s/2$ is referred to as the Nyquist frequency, which leads to aliasing according to the sampling theorem[12]. If noise at 390.038 Hz in the ESU is generated during ECG monitoring, the power of the high frequency is presented at 38 Hz by using sampling frequency of 300 Hz. This result suggests unfiltered noise might appear in the ECG range of 0.5 - 40 Hz. Although almost all modern ECG monitors have a BPF of 0.5 - 40 Hz, the noise signal can be changed and modulated during some signal processing performed by the monitor. Yelderman et al[6] reported that clear ECGs had been obtained with applying ESU when hybrid hardware and software solutions were used.

Fig. 2 shows the frequency spectrum of each ECG as calculated by the DFT. This was done by breaking a whole

ECG signal into 8 segments. Each of these segments is run through a 512-point DFT and the magnitude of the frequency spectra is averaged. It is well known that the resolution and variance of the frequency spectrum depend on the segmental length and the number of segments[12]. When a signal is multiplied by a non-rectangular window before taking the DFT, it is affected regarding resolution and spectral leakage[16]. Since a rectangular window was applied in this study, the resolution is appropriate to calculate the noise reduction ratio at 38 Hz between before and after filtering.

Nimunker and Tompkins[2] showed that most of the frequency content for a real ECG that is taken at a sampling rate of 360 samples/sec lies below 40 Hz. Challis and Kitney[17] also presented frequency response of ECG data which had been sampled at 100 Hz. The results shown in Fig.2A are identical with their findings, and these results agree with previous studies[17, 18].

When a filtered ECG is found by convolving an unfiltered ECG and a filter kernel, the phase can be changed by the filter kernel. This phase shift may cause an error in the results. Challis and Kitney[14] showed that the cross-correlation coefficient can be used to identify simple time delays between events in two signals. The phase in this study also has a difference between window-sinc filter and Chebyshev filters. The correlation coefficient can be applied to quantitative comparison because the 400 samples in the processed ECG are matched with the central portion of the true ECG, which agrees with the gross results (Fig. 4 and Table 3).

This study also shows that the roll-off becomes sharper as the ripple in Chebyshev-type filters increases, which agrees with previous studies[17]. Fig. 3 shows the frequency response of low-pass Chebyshev filter with passband ripples of 0%, 0.6%, 6%, 16%, and 26%. The cut-off frequency of all filters is 0.11 of sampling frequency, which was measured at an amplitude of 0.5. It is important to plot pole locations for filters in the s-plane because the pole location shows the characteristics of the filter[17]. When the ripple percentage is 0, it is called a Butterworth filter. Gregg et al[18] demonstrated that low-pass filtering could result in a significant change in ECG signals. This study also showed that the QRS complex in the ECGs was distorted with the ripple percentage in the 6-pole Chebyshev filters (Fig. 4).

We suggest that the Window-sinc filter performs better than the 6-pole Chebyshev filters for removing 38 Hz noises from ECG signals. Further study is required to implement these results in real-time on an expert monitoring system for clinical practice.

References

1) Christov, II, Iliev GL. Public access defibrillation: suppression of 16.7 Hz interference generated by the power supply of the railway systems. Biomed Eng Online 2005; 4: 16.

2) Nimunkar AJ, Tompkins WJ. EMD-based 60-Hz noise filtering of the ECG. Conf Proc IEEE Eng Med Biol Soc 2007; 2007: 1904-7.

3) van Kleef M, Barendse GA, Kessels A, Voets HM, Weber WE, de Lange S. Randomized trial of radiofrequency lumbar facet denervation for chronic low back pain. Spine 1999; 24: 1937-42.

4) Levkov C, Mihov G, Ivanov R, Daskalov I, Christov I, Dotsinsky I. Removal of power-line interference from the ECG: a review of the subtraction procedure. Biomed Eng Online 2005; 4: 50.

5) Brouse C, Dumont G, Herrmann F, Mark Ansermino J. A Wavelet Approach to Detecting Electrocautery Noise in the ECG. Conf Proc IEEE Eng Med Biol Soc 2005; 1: 788-92.

6) Yelderman M, Widrow B, Cioffi JM, Hesler E, Leddy JA. ECG enhancement by adaptive cancellation of electrosurgical interference. IEEE Trans Biomed Eng 1983; 30: 392-8.

7) Vilos G, Latendresse K, Gan BS. Electrophysical properties of electrosurgery and capacitive induced current. Am J Surg 2001; 182: 222-5.

8) Van Way CW, Hinrichs CS. Electrosurgery 201: basic electrical principles. Curr Surg 2000; 57: 261-4.

9) Smith TL, Smith JM. Electrosurgery in otolaryngology-head and neck surgery: principles, advances, and complications. Laryngoscope 2001; 111: 769-80.

10) Kumar K, Crawford AH. Role of "Bovie" in spinal surgery: historical and analytical perspective. Spine 2002; 27: 1000-6.

11) Massarweh NN, Cosgriff N, Slakey DP. Electrosurgery: history, principles, and current and future uses. J Am Coll Surg 2006; 202: 520-30.

12) Challis RE, Kitney RI. Biomedical signal processing (in four parts). Part 3. The power spectrum and coherence

function. Med Biol Eng Comput 1991; 29: 225-41.

13) Challis RE, Kitney RI. Biomedical signal processing (in four parts). Part 2. The frequency transforms and their inter-relationships. Med Biol Eng Comput 1991; 29: 1-17.

14) Challis RE, Kitney RI. Biomedical signal processing (in four parts). Part 1. Time-domain methods. Med Biol Eng Comput 1990; 28: 509-24.

15) Nelson RM, Ji H. Electric and magnetic fields created by electrosurgical units. IEEE Trans Electromagn Compat 1999; 41: 55-64.

16) Welch PD. The use of fast Fourier transform for the estimation of power spectra: a method based on time averaging over short, modified periodogram. IEEE Trans Audio Electroacoustics 1967; AU-15: 70-3.

17) Challis RE, Kitney RI. The design of digital filters for biomedical signal processing. Part 3: The design of Butterworth and Chebychev filters. J Biomed Eng 1983; 5: 91-102.

18) Gregg RE, Zhou SH, Lindauer JM, Helfenbein ED, Giuliano KK. What is inside the electrocardiograph? J Electrocardiol 2008; 41: 8-14.